Optical Materials 100 (2020) 109627

Contents lists available at ScienceDirect

Optical Materials

journal homepage: http://www.elsevier.com/locate/optmat

Diameter-selected single-walled carbon nanotubes for the passive Q-switching operation at 2 μm

Xiaodong Zhang [a], Hongwei Chu [a,*], Ying Li [b], Shengzhi Zhao [a], Dechun Li [a,**]

[a] School of Information Science and Engineering, Shandong University, Qingdao, 266237, China
[b] Key laboratory of Colloid and Interface Chemistry, Ministry of Education, School of Chemistry and Chemical Engineering, Shandong University, Jinan, 250100, China

ARTICLE INFO

Keywords:
SWCNT saturable absorber
Nonlinear optical response
Q-switching
Liquid phase separation

ABSTRACT

In this paper, we proposed the diameter-selected single-walled carbon nanotubes (SWCNTs) via the simple liquid phase separation for the pulsed 2 μm laser operation as the saturable absorber (SA). The nonlinear absorption properties of the prepared SWCNTs based SA at 2 μm were investigated. The modulation depth and the saturation intensity were 8% and 6.5 kW/cm^2, respectively. By employing the diameter-specified SWCNTs SA, a stable passively Q-switched Tm:YLF laser was demonstrated at 2 μm for the first time. The maximum repetition rate of 35.9 kHz and the shortest pulse duration of 920 ns were achieved with the output coupler of T = 3%. The experiment results indicated that the diameter selection of SWCNTs could be a promising method to improve the Q-switching characteristics.

1. Introduction

The eye-safe solid-state lasers at 2 μm based on Tm^{3+} and Ho^{3+} ions may have potential applications in the atmospheric sounding [1], wind lidar [2], medicine [3], etc. Among these lasers, Q-switching operation at 2 μm is of particular interest owing to the short pulse duration and compactness [4]. Currently, the conventional Q-switches for the pulsed 2 μm lasers include electro-optic modulator (EOM) [5], acoustic-optic modulator (AOM) [6], and semiconductor saturable absorber mirrors (SESAMs) [7–9]. As the active modulator, both EOM and AOM require the sophisticated electronic control systems. While for SESAMs, the main drawbacks are the complex design, precisely controlled fabrication and the huge expenses [10]. Considering the essential role of the saturable absorbers in the Q-switching and mode-locking operation, novel saturable absorbers at 2 μm with high performance are still the ultimate goal.

Even discovered in 1991 [11], carbon nanotubes (CNTs), especially the single walled carbon nanotubes (SWCNTs) still attract much attention in recent years [12]. The mixture or randomly aligned SWCNTs can provide broad absorption band spanning from 0.5 μm up to 2.8 μm [13], which strongly depends on the diameter of SWCNTs [14]. In addition, SWCNTs exhibit the wideband nonlinear absorption and the ultrafast (about 1 ps) recovery time, which are suitable for the passive Q-switching and mode-locking operations [15–17]. In fact, with respect to SWCNTs, the main mechanism of the saturable absorption is the interband energy transition, i.e. so-called van Hove singularity (vHs) transitions (E_{11}) [18]. Because of the direct band structure of SWCNTs, the strongest saturable absorption appears when the E_{11} resonate wavelength matches the laser wavelength [14]. Thus, sorting the diameter of SWCNTs is the main task for the optimization of saturable absorption properties. For the SWCNTs based SA, the reasonable diameter should be around 1.7 nm for 2 μm lasers according to the Kataura plot [19,20]. However, up to date, the sorting method of SWCNTs with a large diameter (>1.5 nm) is still unreliable and low efficient.

In the present work, we proposed a simple liquid phase separation method to select the SWCNTs with the diameter around 1.7 nm. The nonlinear optical performance of SWCNTs based SA was investigated by an open aperture Z scan setup. The modulation depth was 8% while the saturation intensity was 6.5 kW/cm^2, which is suitable for the Q-switching operation at 2 μm. As an application, the diameter-selected SWCNTs saturable absorber Q-switched Tm:YLF laser was demonstrated at 1906 nm, producing the minimum pulse duration of 920 ns with a pulse repetition rate of 35.9 kHz.

* Corresponding author.
** Corresponding author.
E-mail addresses: hongwei.chu@sdu.edu.cn (H. Chu), dechun@sdu.edu.cn (D. Li).

https://doi.org/10.1016/j.optmat.2019.109627
Received 5 November 2019; Received in revised form 29 November 2019; Accepted 18 December 2019
Available online 26 December 2019
0925-3467/

2. Preparation and characterization of SA

SWCNTs powder with diameter range from 1 to 2 nm was grown via the catalytic CVD (XFNano Cor., China). 5 mg SWCNT powder was poured into 10 mL 1% sodium dodecyl sulfate (SDS) aqueous solution to prepare the SWCNT aqueous solution at first. And the solution with excellent dispersibility was obtained after ultrasonically agitating for 2 h. The dispersed SWCNTs solution was centrifuged for 10 min at 3000G to remove bundles and efficiently obtain the SWCNTs with large diameter. The supernatant part was transferred on a UV fused silica (UVFS) substrate and dried in an oven at 60 °C. As a consequence, the SWCNTs SA was fabricated. In order to make sure the E_{11} transition at 2 μm, we measured the absorption spectrum of the prepared diameter-specified SWCNTs SA. As shown in Fig. 1, there is a significant enhanced absorption band near 2 μm, indicating that the SWCNTs with the diameter of ~1.7 nm were successfully selected.

The morphology of the prepared SWCNTs on the UFVS substrate was investigated using the atomic force microscopy (AFM). The AFM working at the tapping mode was used to probe the height distribution. As shown in Fig. 2, three different positions are chosen for the height statistics. The size distribution of the fabricated SWCNTs was mostly in the range from about 1.6 to 1.7 nm. Both AFM morphology and the absorption spectrum confirmed that the as-prepared SWCNTs possessed the diameter of ~1.7 nm.

A typical open-aperture Z-scan system was applied to characterize the nonlinear optical performance of the prepared SWCNTs based SA. Fig. 3 shows the schematic setup of the open-aperture Z scan experiment. The excitation source was an AOM Q-switched Tm:YLF laser with a pulse duration of 260 ns at the pulse repetition rate of 1 kHz. A balanced measurement was employed in our case. The laser beam was separated by a 50:50 beam splitter. One beam was the reference and the other on was to excite the SWCNTs sample. The lens with a focal length of 270 mm was utilized.

Fig. 4(a) displays the normalized transmission data from the open-aperture Z-scan experiment, indicating that the prepared SWCNTs possessed the typical saturable absorption behavior at the incident intensity of I_0 = 31.3 kW/cm^2. As shown in Fig. 4(b), the nonlinear transmission performance of SWCNT-SA was investigated. The nonlinear absorption behavior of a saturable absorber that depends on the intensity of the incident beam was fitted (Fig. 4(b)) by using the following simple formula [21]:

$$T(I) = 1 - \Delta R \exp(-I/I_{sat}) - R_s \tag{1}$$

where $T(I)$ is the transmission, ΔR is the modulation depth, I is the pulse intensity, I_{sat} is the saturation intensity, and R_s is the non-saturable loss. According to the fitting, the modulation depth was 8% and the saturation intensity was 6.5 kW/cm^2.

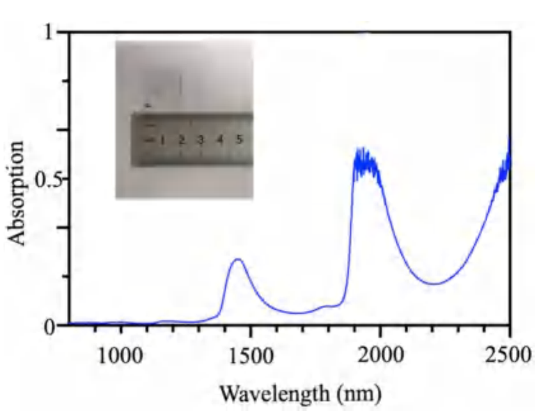

Fig. 1. The absorption spectrum of the prepared SWCNTs SA. Inset: Picture of SWCNTs SA on UVFS substrate.

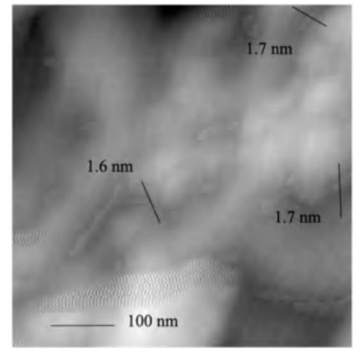

Fig. 2. The AFM morphology of the prepared SWCNT-SA.

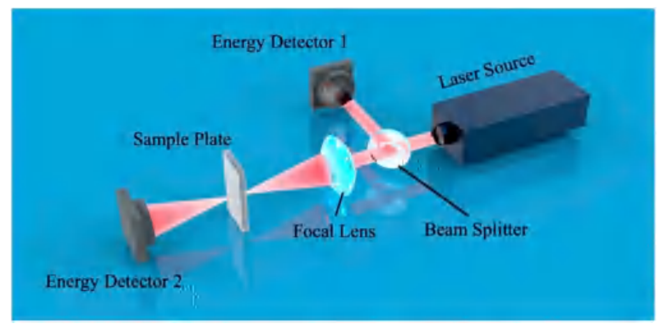

Fig. 3. The schematic setup of the open-aperture Z scan.

3. Passively Q-switched Tm:YLF laser

The passively Q-switched Tm:YLF solid laser experiment was conducted. The experimental setup is schematically displayed in Fig. 5. The pump supply was a 794 nm fiber-coupled laser diode with a diameter of 400 μm and a numerical aperture (NA) of 0.22. The pump laser was focused on the crystal by using a 1:1 imaging optics. The input mirror M1 was AR-coated at 794 nm and HR-coated at 1.9 μm. A polished 3 mm × 3 mm × 10 mm Tm:YLF crystal with a doping concentration of 2 at.% was used as the gain medium in this work, which was wrapped by the indium foil and cooled by a copper heatsink. The crystal temperature was set at 15 °C to reduce the thermal effect. In our case, two output couplers (OCs) with T = 1% and T = 3% at 1.9 μm were chose. The SWCNT based SA was inserted into the laser resonator near the OC M2. The whole length of the laser cavity was 15 mm. A laser power matter (S470C, Thorlabs, USA), a high-performance digital oscilloscope (2 GHz bandwidth and 5 G samples/s sampling rate, Tektronix Inc., USA) and a homemade fast InGaAs photodiode detector (with a rise time 1 ns) were used to recording the pulsed laser output performance.

Initially, we investigated the output characteristics with an OC of T = 1% at 1.9 μm. As shown in Fig. 6(a), the maximum continues-wave (CW) output power is 435 mW at the highest pump power of 2.5 W. For the passive Q-switching (PQS) operation, the maximum power was 63 mW. The slope efficiencies of CW and PQS operations were 23.3% and 4.2%, respectively. When the SWCNTs based SA was inserted into the laser cavity, stably passively Q-switched Tm:YLF laser was obtained. As the launched pump power increased from 1.2 to 2.5 W, the pulse duration decreased from 1527 ns to 960 ns. While the pulse repetition rate performed huge fluctuations, which may be contributed to the significant thermal effect and the optical scattering of the un-uniform SA surface. We believed that a better SA fabrication method would lead to the better repetition rate performance. And the shortest pulse duration of 960 ns and the pulse train at the highest pulse repetition frequency of 29.4 kHz were shown in Fig. 6(c) and 6(d), respectively. The relatively long pulse width may come from the low gain in the resonator since the

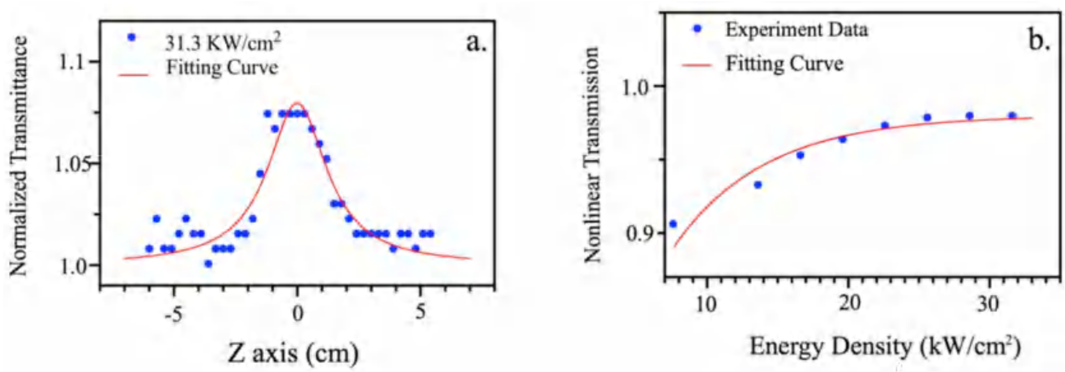

Fig. 4. (a) The Z scan curve with the incident peak intensity of 31.3 kW/cm^2; (b) The nonlinear transmission of SA.

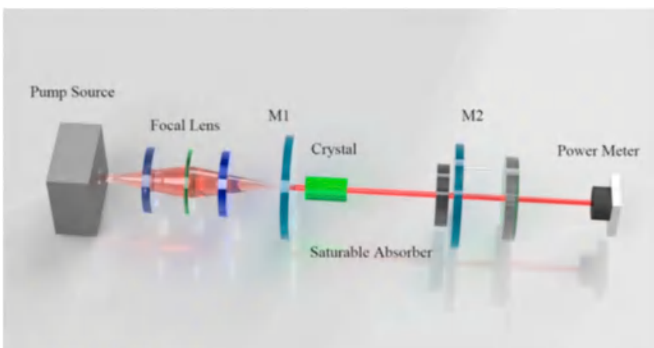

Fig. 5. The passively Q-switched Tm:YLF laser setup.

pump level was very low. In addition, due to the bundles of the prepared SWCNTs SA would also lead to the high saturable intensity and long buildup time of the pulses.

Then another OC of T = 3% was exploited in the experiment. Fig. 7 (a) displays the CW and PQS output powers versus the pump power. The slope efficiency of them are 25% and 4.6%, respectively. Under the pump level of 1.93 W, the maximum CW output power was 281 mW while for the PQS operation, the highest output power was about 38 mW. The pulse duration and the pulse repetition frequency versus pump power were given in Fig. 7(b). The pulse width decreased to 920 ns with the increase of the incident pump power. As a counterpart, the repetition frequency augmented to 35.9 kHz. Notably, we did not further increase the pump power since the pulse became unstable when the pump power was beyond 2 W. The typical temporal profile of the shortest pulses was demonstrated in Fig. 7(c), the corresponding pulse train was shown in Fig. 7(d), demonstrating the relative stable Q-switching operation. We noted that the pulse duration (920 ns) from the laser resonator with an OC of T = 3% was slightly shorter. Indeed, the slope efficiency was also higher, indicating the large gain in the laser cavity. It is no doubt that the large gain in the laser resonator would benefit the narrower pulses.

4. Conclusion

In summary, the SWCNTs with the specific diameter (>1.5 nm) was sorted with the simple liquid-phase separation method. The nonlinear optical properties were measured by an open-aperture Z-scan technique,

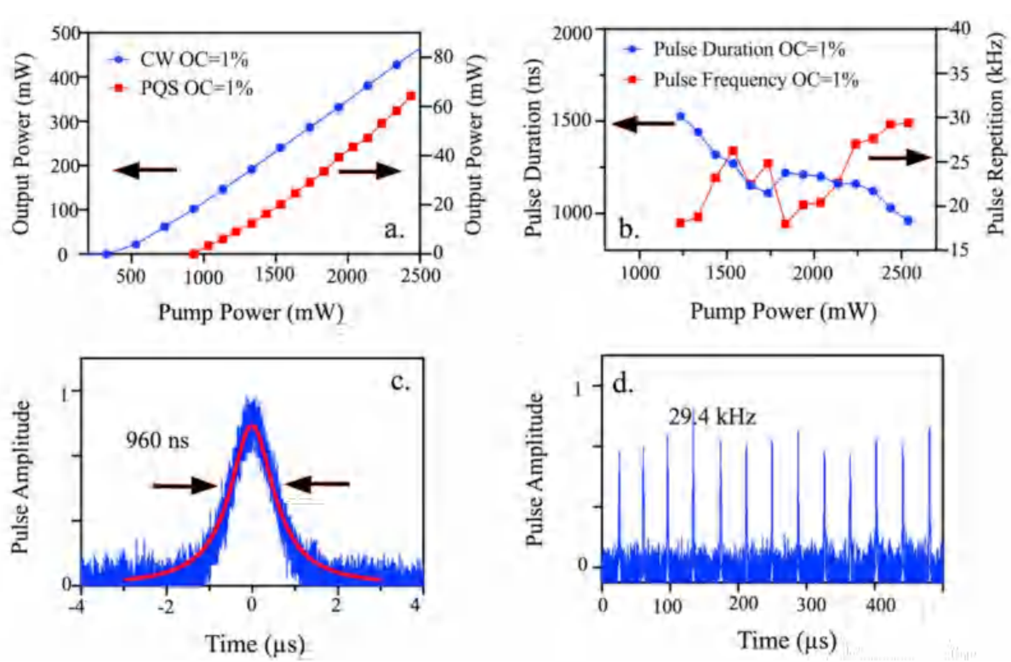

Fig. 6. (a) The CW output power (blue dots) and the Q-switching (PQS) output power (red dots) with OC of 1% versus pump power; (b) The pulse duration (blue dots) and the pulse repetition frequency (red dots) with OC of 1% versus pump power; (c) The temporal profile of 960 ns; (d) The pulse train of 29.4 kHz. (For interpretation of the references to colour in this figure legend, the reader is referred to the Web version of this article).

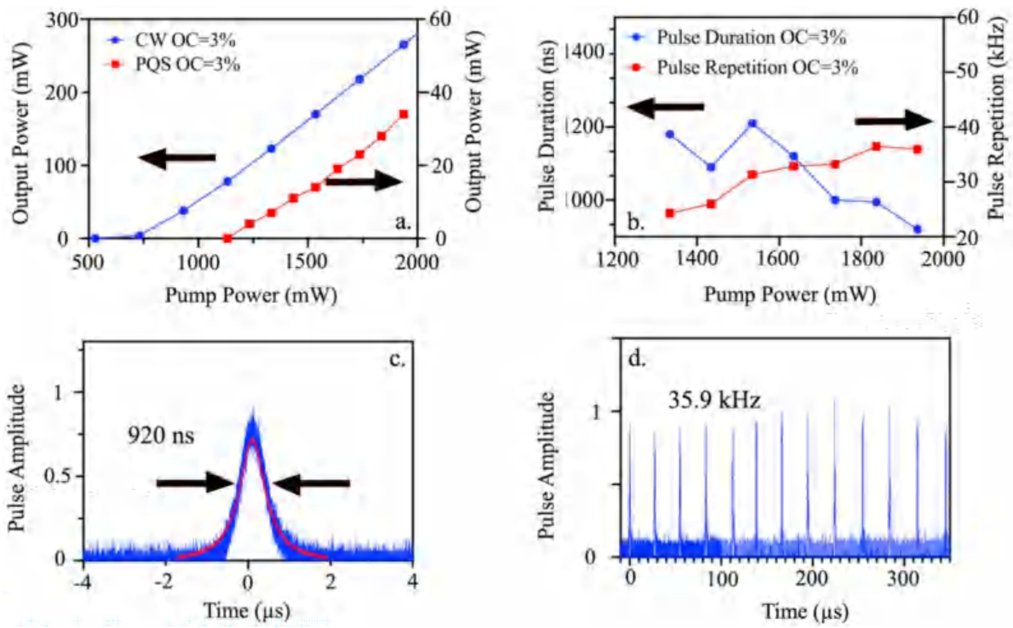

Fig. 7. (a) The CW output power (blue dots) and the PQS output power (red dots) with OC of 3% versus pump power; (b) The pulse duration (blue dots) and the pulse repetition frequency (red dots) versus the pump power; (c) The temporal profile of 920 ns; (d) The pulse train of 35.9 kHz. (For interpretation of the references to colour in this figure legend, the reader is referred to the Web version of this article).

and the modulation depth of 8% and the saturation intensity were 6.5 kW/cm^2 were obtained. With the diameter-selected SWCNTs based saturable absorber, a stable passively Q-switched Tm:YLF laser was realized at 2 μm with the maximum repetition rate of 35.9 kHz and the shortest pulse duration of 920 ns. Our results verified that the diameter-selected SWCNTs saturable absorber could be suitable for the Q-switching operation at the resonant wavelength of E_{11} transition.

Author contributions section

XZ performed the experiment and the characterization; YL analyzed the experimental data; SZ helped in the laser experiment; HC and DL conceived the idea and co-supervised the whole project. All authors discussed the manuscript.

Declaration of competing interest

The authors declare that they have no known competing financial interests or personal relationships that could have appeared to influence the work reported in this paper.

Acknowledgement

The authors thank the financial support of the National Natural Science Foundation of China (NSFC, 61575109 and 21872084) and Fundamental Research Funds of Shandong University (2018TB044).

References

[1] G.J. Koch, A.N. Dharamsi, C.M. Fitzgerald, J.C. McCarthy, Frequency stabilization of a Ho: Tm: YLF laser to absorption lines of carbon dioxide, Appl. Opt. 39 (21) (2000) 3664–3669.
[2] B.T. McGuckin, R.T. Menzies, H. Hemmati, Efficient energy extraction from a diode-pumped Q-switched Tm, Ho: YLiF4 laser, Appl. Phys. Lett. 59 (23) (1991) 2926–2928.
[3] Q. Zun-Shi, W. Yong-Gang, L. Jie, Z. Li-He, S. Liang-Bi, X. Jun, Passively mode-locked 2-μm Tm: YAP laser with a double-wall carbon nanotube absorber, Chin. Phys. B 21 (6) (2012), 064211.
[4] A.A. Lagatsky, F. Fusari, S. Calvez, J.A. Gupta, V.E. Kisel, N.V. Kuleshov, W. Sibbett, Passive mode locking of a Tm, Ho: KY (WO 4) 2 laser around 2 μm, Opt. Lett. 34 (17) (2009) 2587–2589.
[5] A.F. El-Sherif, T.A. King, High-energy, high-brightness Q-switched Tm3+-doped fiber laser using an electro-optic modulator, Opt. Commun. 218 (4–6) (2003) 337–344.
[6] B. Yao, Y. Tian, G. Li, Y. Wang, InGaAs/GaAs saturable absorber for diode-pumped passively Q-switched dual-wavelength Tm: YAP lasers, Opt. Express 18 (13) (2010) 13574–13579.
[7] J.L. Xu, X.L. Li, J.L. He, X.P. Hao, Y. Yang, Y.Z. Wu, B.T. Zhang, Efficient graphene Q switching and mode locking of 1.34 μm neodymium lasers, Opt. Lett. 37 (13) (2012) 2652–2654.
[8] J.L. Xu, X.L. Li, Y.Z. Wu, X.P. Hao, J.L. He, K.J. Yang, Graphene saturable absorber mirror for ultra-fast-pulse solid-state laser, Opt. Lett. 36 (10) (2011) 1948–1950.
[9] Q. Bao, H. Zhang, Y. Wang, Z. Ni, Y. Yan, Z.X. Shen, D.Y. Tang, Atomic-layer graphene as a saturable absorber for ultrafast pulsed lasers, Adv. Funct. Mater. 19 (19) (2009) 3077–3083.
[10] D. Popa, Z. Sun, F. Torrisi, T. Hasan, F. Wang, A.C. Ferrari, Sub 200 fs pulse generation from a graphene mode-locked fiber laser, Appl. Phys. Lett. 97 (20) (2010) 203106.
[11] S. Iijima, Helical microtubules of graphitic carbon, Nature 354 (6348) (1991) 56.
[12] A. Martinez, Z. Sun, Nanotube and graphene saturable absorbers for fibre lasers, Nat. Photonics 7 (11) (2013) 842.
[13] S.M. Bachilo, M.S. Strano, C. Kittrell, R.H. Hauge, R.E. Smalley, R.B. Weisman, Structure-assigned optical spectra of single-walled carbon nanotubes, Science 298 (5602) (2002) 2361–2366.
[14] W.B. Cho, J.H. Yim, S.Y. Choi, S. Lee, A. Schmidt, G. Steinmeyer, F. Rotermund, Boosting the non linear optical response of carbon nanotube saturable absorbers for broadband mode-locking of bulk lasers, Adv. Funct. Mater. 20 (12) (2010) 1937–1943.
[15] S. Yamashita, Nonlinear optics in carbon nanotube, graphene, and related 2D materials, APL Photonics 4 (3) (2019), 034301.
[16] A. Schmidt, S. Rivier, G. Steinmeyer, J.H. Yim, W.B. Cho, S. Lee, F. Díaz, Passive mode locking of Yb: KLuW using a single-walled carbon nanotube saturable absorber, Opt. Lett. 33 (7) (2008) 729–731.
[17] P. Loiko, X. Mateos, S.Y. Choi, F. Rotermund, J.M. Serres, M. Aguiló, V. Petrov, Vibronic thulium laser at 2131 nm Q-switched by single-walled carbon nanotubes, JOSA B 33 (11) (2016) D19–D27.
[18] S.M. Bachilo, M.S. Strano, C. Kittrell, R.H. Hauge, R.E. Smalley, R.B. Weisman, Structure-assigned optical spectra of single-walled carbon nanotubes, Science 298 (5602) (2002) 2361–2366.
[19] S.Y. Set, H. Yaguchi, Y. Tanaka, M. Jablonski, Ultrafast fiber pulsed lasers incorporating carbon nanotubes, IEEE J. Sel. Top. Quantum Electron. 10 (1) (2004) 137–146.
[20] R.B. Weisman, S.M. Bachilo, Dependence of optical transition energies on structure for single-walled carbon nanotubes in aqueous suspension: an empirical Kataura plot, Nano Lett. 3 (9) (2003) 1235–1238.
[21] H. Pan, H. Chu, Y. Li, S. Zhao, D. Li, Comprehensive study on the nonlinear optical properties of few-layered MoSe2 nanosheets at 1 μm, J. Alloy. Comp. 806 (2019) 52–57.